

1 A model for predicting smoke back-layering length in tunnel  
2 fires with the combination of longitudinal ventilation and  
3 point extraction ventilation in the roof

4 Junheng Wang<sup>a,b,c</sup>, Jianping Yuan<sup>a,b</sup>, Zheng Fang<sup>a,b</sup>, Zhi Tang<sup>a,b,\*</sup>, Peng Qian<sup>c</sup>, Jianqiao  
5 Ye<sup>a,c</sup>

6 <sup>a</sup> School of Civil Engineering, Wuhan University, Wuhan 430072, China

7 <sup>b</sup> Engineering Research Centre of Urban Disasters Prevention and Fire Rescue Technology of Hubei  
8 Province, Wuhan 430072, China

9 <sup>c</sup> Department of Engineering, Lancaster University, Lancaster LA1 4YR, U.K.

10 **Abstract:** An analytical model is developed for quantifying the fire smoke back-layering length in a tunnel with  
11 a combination of longitudinal ventilation and point extraction ventilation in the roof. The distance of smoke vent  
12 to fire source is incorporated as well as mass flow rate during the whole smoke flow process according to the  
13 mass conservation principle. The model input quantities are the heat release rate of the fire source, the  
14 longitudinal velocity, the exhaust velocity, the width and the height of the tunnel, the distance of the smoke vent  
15 to the fire source and the area of the smoke vent. The quality of the model predictions is illustrated for a range of  
16 experimental conditions. After that, extensive model predictions on the back-layering length are presented to  
17 show its trends by varying the velocity of the longitudinal ventilation, the exhaust velocity and the position of  
18 the smoke vent in the roof. Discussions are given at last. It is highlighted that shortening the distance between  
19 the smoke vent and the fire source benefits shortening the back-layering length, and this phenomenon is more  
20 pronounced for higher exhaust velocity.

---

\*Corresponding author. Tel.: +86 027 68772312

E-mail address: zhi.tang@whu.edu.cn (Zhi Tang) .

**Nomenclature**

$A$	area of the smoke vent, $m$	$V^{**}$	modified dimensionless longitudinal velocity
$A_t$	cross-sectional area of the tunnel, $m^2$		longitudinal velocity induced by
$B$	tunnel width, $m$	$V'$	both the longitudinal ventilation and the point extraction, $m/s$
$C$	coefficient constant	$V_a$	longitudinal velocity induced by the longitudinal ventilation, $m/s$
$c_p$	specific heat capacity, $kJ/(kg \cdot K)$	$V_c$	critical velocity, $m/s$
$d$	distance from smoke vent to fire source, $m$	$w^*$	characteristic plume velocity, $m/s$
$D$	contact length, $m$	$x$	coordinate at the virtual x-axis, $m$
$D'$	characteristic length		coordinate of the position of the
$Fr$	Froude number	$x_0$	maximum excess ceiling temperature, $m$
$Fr_m$	modified Froude number		
$g$	gravitational acceleration, $m/s^2$		
$h$	smoke layer height, $m$		
$H$	tunnel height, $m$		
$H_d$	height from fire source to tunnel ceiling, $m$		
$K$	longitudinal decay coefficient of the ceiling excess temperature		
$K'$	modified longitudinal decay coefficient of the ceiling excess temperature		
	longitudinal decay coefficient of the ceiling excess temperature downstream the smoke vent		
$K_1$	longitudinal decay coefficient of the ceiling excess temperature downstream the smoke vent		
$l$	back-layering length, $m$		
$l'$	the second part of back-layering length, $m$		
$l^*$	dimensionless back-layering length		
$l^{**}$	modified dimensionless back-layering length		
$\dot{m}$	plume mass flow rate, $kg \cdot s$		
$\dot{Q}_c$	convective heat release rate, $kW$		
$\dot{Q}$	heat release rate, $kW$		
$\dot{Q}^*$	dimensionless heat release rate		
$\dot{Q}^{**}$	modified dimensionless heat release rate		
$r$	radius of the fire source, $m$		
$Ri'$	modified Richardson number		
$T$	temperature, $K$		
$V$	velocity, $m/s$		
$V^*$	dimensionless longitudinal velocity		

**Greek symbols**

$\alpha$	heat transfer coefficient
$\gamma$	experiments coefficient
$\varepsilon$	experiments coefficient
$\rho$	density, $kg/m^3$
$\theta$	flame angle, $^\circ$
$\Delta$	excess over the initial value
$\delta$	proportional coefficient

**Subscript**

0	initial value
a	ambient
ex	exhaust
in	induced
max	max value
r	residual
s	stagnation
up	upstream

24 **1. Introduction**

25 In the last few decades, tunnel fires have caused a lot of damage to properties and casualties  
 26 [1-3], and the fire smoke is the leading reason. The danger of the smoke in tunnel fire not  
 27 only results from the visibility obscuring effect but also from its toxicity. The ventilation

28 systems are then applied in tunnels to deal with the fire smoke and the longitudinal  
29 ventilation system is a common one. The principle of the longitudinal ventilation is to blow  
30 the fire smoke to the downstream of the fire source so that the upstream side would be clear  
31 for evacuation and rescue. However, sometimes the longitudinal air flow would be smaller  
32 than the critical velocity due to the poor ventilation capability, large fire scale or the  
33 “throttling effect”. As a result, the smoke would spread upstream of the fire source and then  
34 the back-layering (upstream traveling of the smoke in the direction opposite to the ventilation)  
35 occurs. Apparently, the smoke back-layering would danger the evacuees and the rescuers  
36 upstream of the fire and lead to an increase in number of casualties in tunnel fires. So it is  
37 significant to study and quantify the back-layering length in the case of the tunnel fire.

38 Many scholars have developed models for quantifying the back-layering length, but most of  
39 them were developed in the contexts of the tunnels with the longitudinal ventilations. Because  
40 of destroying the stratification of the smoke downstream of the fire source, the limitation in  
41 the use of the longitudinal ventilation system is apparent. The longitudinal ventilation is  
42 preferably applied to non-congested tunnels where there are normally no people downstream  
43 of the fire source. As for the urban tunnels designed for queues, it is a challenge to only adopt  
44 a sole longitudinal ventilation system. To take this challenge, the longitudinal ventilation is  
45 often designed together with the extraction ventilation in Chinese urban tunnels (e.g. Wuhan  
46 Yangtze River tunnel and Nanjing Yangtze River tunnel). When a fire occurs, the smoke vent  
47 closed to the fire source would open to assist in exhausting the fire smoke. It is no doubt that  
48 the point extraction ventilation in the roof would interact with the longitudinal ventilation  
49 system to affect the formation of the smoke back-layering. Present paper will focus on this  
50 phenomenon and build a model to quantify the length of the back-layering under the  
51 combined effect of the longitudinal ventilation and the point extraction ventilation in the roof.

52 The structure of this paper is as follows. A review of the models for quantifying smoke back-  
 53 layering flow length is presented firstly. Then, the phenomenon described by the model is  
 54 introduced before the introduction of the phenomenon described by the model. Next, the  
 55 accuracy of the model for predicting the back-layering length is illustrated by means of the  
 56 experimental data and a third party model. Afterwards, the influences of the longitudinal  
 57 velocity, the exhaust velocity and the distance of the smoke vent from the fire source on the  
 58 back-layering length are discussed, and some conclusions are made at last.

## 59 **2. Literature review**

60 In the previous research, many models [4-8] have been developed to predict the length of  
 61 back-layering. However, most of them are aim to serve for the purely longitudinal ventilated  
 62 tunnels, and a few studies consider the contexts of the combination of the longitudinal  
 63 ventilation and the point extraction ventilation in the roof.

64 In 1958, a theory of describing the back-layering length was proposed by Thomas[8] in  
 65 1958. In [8], the dimensionless back-layering length,  $l^*$ , was correlated with a modified  
 66 Froude number,  $Fr_m = \frac{gH\Delta T}{V_a^2(T_a+\Delta T)}$ . The proposed relation was expressed as follows:

$$67 \quad l^* = \frac{l}{H} \propto \frac{gFr_m}{\rho_a c_p V_a \Delta T A_t} \quad (1)$$

68 where  $g$  is the gravitational acceleration,  $H$  is the tunnel height,  $\rho_a$  is ambient air density,  $c_p$   
 69 is the specific heat capacity of air,  $l$  is the back-layering length,  $V_a$  is the longitudinal velocity,  
 70  $A_t$  is the cross-sectional area of the tunnel,  $T_a$  is the ambient temperature.  $\Delta T$  is the  
 71 temperature excess over ambient.

72 In 1991, Vantelon et al. [5] defined a modified Richardson number,  $Ri' = \frac{gQ_0}{\rho_a T_a c_p V_a^3 H}$ , and  
 73 proposed that the dimensionless back-layering length varied as 0.3 power of  $Ri'$ , given as:

74 
$$l^* \propto Ri'^{0.3} \quad (2)$$

75 where  $\dot{Q}_0$  is the heat release rate of the fire source.

76 In 2001, based on the experiments performed in a model tunnel of Paris metro, Deberteix et  
 77 al. [7] correlated the back-layering length with the Richardson number,  $Ri = \frac{gD'\Delta T}{V_a^2 T_a}$ , to  
 78 proposed the equation as follows:

79 
$$l^* = 7.5(Ri^{1/3} - 1) \quad (3)$$

80 where  $D'$  is a characteristic length.

81 In 2010, Li and Ingason et al. [6] performed small-scale experiments and correlated the  
 82 dimensionless smoke back-layering length to the dimensionless heat release rate of the fire  
 83 source and the dimensionless longitudinal velocity. The correlation shows as follows:

84 
$$l^* = \begin{cases} 18.5 \ln(0.81 \dot{Q}^{*1/3} / V^*), & \dot{Q}^* \leq 0.15 \\ 18.5 \ln(0.43 / V^*), & \dot{Q}^* > 0.15 \end{cases} \quad (4)$$

85 where

86 
$$l^* = \frac{l}{H}$$

87 (5)

88 
$$V^* = \frac{V_a}{\sqrt{gH}}$$

89 (6)

90 
$$\dot{Q}^* = \frac{\dot{Q}_0}{\rho_a c_p T_a g^{1/2} H^{5/2}}$$

91 (7)

92 Considering the driving force of the fire smoke, the upstream smoke flow should stop at the  
 93 place where the static pressure balances to the dynamic pressure caused by the longitudinal

94 ventilation. Based on this theory, Chow et al. [4] studied the back-layering length in a tilted  
 95 tunnel with longitudinal ventilation, and calculated the back-layering length with the ceiling  
 96 temperature. The expression gives as:

$$97 \quad l = -\frac{1}{K} \ln \left[ \frac{V_a^2}{gh_0} \frac{1}{\gamma (\dot{Q}^{*2/3} / Fr^{1/3})^\varepsilon} \right] \quad (8)$$

98 where  $\gamma$ ,  $\varepsilon$  are coefficients obtained by the experiments [9],  $K$  is the longitudinal decay  
 99 coefficient of the ceiling excess temperature,  $h_0$  is the initial smoke layer height,  $Fr$  is the  
 100 Froude number.

101 Apart from the models introduced above, Hu et al. [10] developed models of quantifying the  
 102 back-layering length for the purely longitudinal ventilated tunnels. Along with the same  
 103 research methodologies as described previously, some scholars tried to study the effect of the  
 104 point extraction by the smoke vent on the back-layering. Vauquelin et al. [11, 12]  
 105 experimentally investigated the smoke flow profiles in a scaled tunnel with a point extraction  
 106 system and defined the “confinement velocity” at which the smoke layering length would be  
 107 confined to be certain value by the induced wind. Ingason and Li [13] conducted small-scale  
 108 experiments to study the single point and two-point extraction system combining with the  
 109 longitudinal ventilation or the natural ventilation handling with the HGV fires. Chen et al.  
 110 [14] established a mathematical model to predict the two-directional smoke back-layering  
 111 length with a combination of the point extraction and the longitudinal ventilation. In that  
 112 work, a smoke vent was set just above the fire source. The correlations were expressed as:

$$113 \quad l^{**} = \begin{cases} 18.5 \ln(0.81 \dot{Q}^{**1/3} / V^{**}), & \dot{Q}^{**} \leq 0.15 \\ 18.5 \ln(0.43 / V^{**}), & \dot{Q}^{**} > 0.15 \end{cases} \quad (9)$$

114 With

115 
$$\dot{Q}^{**} = \frac{\dot{Q}_0 - c_p \rho_{ex} V_{ex} A \Delta T_{max}}{\rho_a c_p T_a g^{1/2} H^{5/2}}$$

116 (10)

117 
$$l^{**} = \frac{l}{H}$$

118 (11)

119 and

120 
$$V^{**} = \frac{V_a + \rho_{ex} V_{ex} A / 2BH \rho_a}{\sqrt{gH}} \quad \text{for the upstream}$$

121 (12)

122 
$$V^{**} = \frac{\rho_{ex} V_{ex} A / 2BH \rho_a - V_a}{\sqrt{gH}} \quad (V_a < \rho_{ex} V_{ex} A / 2BH \rho_a) \quad \text{for the downstream}$$

123 (13)

124 where  $\rho_{ex}$  is the density of exhaust smoke,  $V_{ex}$  is the exhaust velocity,  $A$  is the area of smoke  
 125 vent,  $\Delta T_{max}$  is the maximum temperature excess the ambient,  $B$  is the tunnel width.

126 However, the fire does not always occur just below the smoke vent. Chen et al. [15] further  
 127 carried out experiments with the smoke vent at different downstream distance from the fire  
 128 source. The previously established mathematical model (Eq.9) [14] was also able to predict  
 129  $l^{**}$  in the contexts of the smoke vent locating downstream of the fire source by giving:

130 
$$\dot{Q}^{**} = \frac{\dot{Q}_0 - c_p \rho_{ex} V_{ex} A \Delta T_{max} e^{-Kd}}{\rho_a c_p T_a g^{1/2} H^{5/2}} \quad (14)$$

131 where  $d$  is the distance from smoke vent to the fire source.

132 Models in both [14] and [15] describe the smoke vent located just above the fire source and at  
 133 the downstream side respectively. In fact, the smoke vent upstream of the fire source would  
 134 be operated as well. As a consequence, the smoke vent upstream of the fire source might  
 135 directly exhaust the smoke from the smoke back-layering, so that the back-layering length

136 would be different from the situation that the smoke vent is operating at the downstream side  
 137 [15]. And it had been confirmed by the experiments conducted by Tang et al. [16]. In their  
 138 experimental configuration [16], the smoke vent was set upstream of the fire source  
 139 compared to the experiments conducted by Chen et al. [15]. The experiment results observed  
 140 by Tang et al. [16] highlighted that the smoke back-layering length in their experiments was  
 141 shorter than that from experiments conducted by Chen et al. [15]. Based on the experimental  
 142 data, they proposed a modified longitudinal decay coefficient of the ceiling excess  
 143 temperature ( $K'$ ) in the model of Chen et al. [15] (Eq.14):

$$144 \quad K' = \left( \frac{V_c}{V_c - V_a} \right)^{0.3} \times \frac{\alpha D}{c_p (0.071 \dot{Q}_0^{1/3} H_d^{5/3} - \dot{m}_{ex})} \quad (15)$$

145 where  $V_c$  is the critical velocity,  $\alpha$  is the heat transfer coefficient,  $H_d$  is the height from the  
 146 fire source to tunnel ceiling,  $\dot{m}_{ex}$  is the mass flow rate of the exhaust smoke .

147 Yao et al.[17] have done similar experimental work, focusing on the smoke back-layering  
 148 flow length in the longitudinal ventilated tunnel with vertical shaft by the natural ventilation  
 149 on the upstream side of the fire source. They also proposed a modified prediction model  
 150 derived from the model of Li et al. [6].

151 As already reviewed, there are many literatures focusing on the smoke back-layering length,  
 152 but the relevant research on the smoke back-layering in the contexts of the combination of the  
 153 longitudinal ventilation and the point extraction ventilation was not many found. The existing  
 154 models for quantifying these phenomenon [14-16] were all based on the model proposed by  
 155 Li et al. [6], deriving from the dimensionless correlation between the smoke back-layering  
 156 length and the longitudinal velocity. The effect of the point extraction ventilation on the  
 157 back-layering was considered by introducing a reduced heat release rate of the fire source,  
 158  $\dot{Q}^{**}$ , from the point view of the heat conservation. However, the mass conservation during

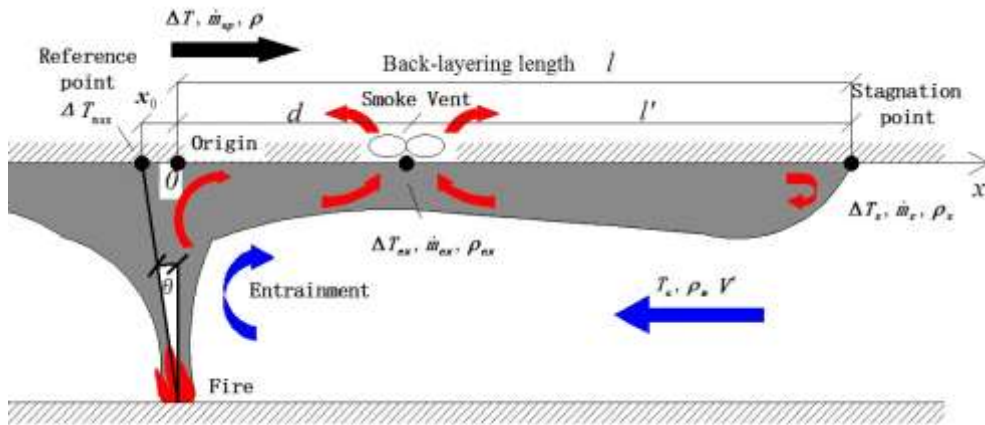


159 the whole spread process of the back-layering was not incorporated into the existing models  
160 yet. As it is obviously that the mass flow rate is an important parameter for the formation of  
161 the back-layering, particularly for the mass flow rate changing at the smoke vent position, a  
162 model would be developed in this research to take this challenge. More specifically, the  
163 smoke back-layering is divided into two regions by the smoke vent, and the whole process of  
164 smoke spreading through the smoke vent is considered in the model development based on  
165 mass and energy conservation principles.

### 166 **3. Model development**

167 Fig. 1 shows the sketch of the phenomenon described in the model. There is a fire occurring  
168 in a tunnel, and a smoke back-layering is formed upstream of the fire source. The smoke  
169 back-layering is suppressed by the combined effect of the longitudinal ventilation and the  
170 point extraction ventilation in the roof upstream of the fire source, because the fire smoke  
171 would be blown to the downstream by the longitudinal air flow and be extracted out of the  
172 tunnel by the smoke vent in the roof. A virtual x-axis is introduced and the origin is set just  
173 above the fire source. Fig. 1 also displays the distance between the smoke vent and the fire  
174 source,  $d$ , and the stagnation point where is the smoke back-layering stopping propagating.

175 Indeed, the process of the smoke spreading in the tunnel as shown in Fig.1, is similar to the  
176 smoke propagation in the tunnel with the longitudinal ventilation, apart from that partial  
177 smoke being removed by the smoke vent which is immersed in the smoke back-layering.  
178 Consequently, it is logical that the model for quantifying the back-layering length in Fig. 1  
179 can be developed in a similar way to the models only taking the longitudinal ventilation  
180 system into account. According to Fig.1, the back-layering length can be divided into two  
181 parts: (1) the smoke flow length between the smoke vent and the origin (the fire source); (2)  
182 the smoke flow length between the smoke vent and the stagnation point.



183

184 Fig.1 Schematic diagram of the fire smoke spreading with the point extraction ventilation and the longitudinal  
 185 ventilation

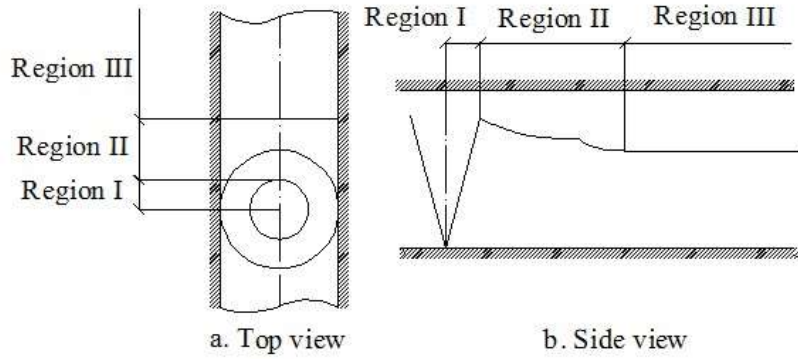
186 The first part of the back-layering length equals to the distance between the smoke vent and  
 187 the fire source,  $d$ .

188 The second part of the back-layering length is the length of the smoke flow that begins from  
 189 the position of the smoke vent. Thus the second part of the smoke back-layering length can  
 190 be determined by the smoke characteristics (e.g. the smoke mass flow rate and the  
 191 temperature) at the position of the smoke vent and the longitudinal velocity induced by both  
 192 of the longitudinal ventilation and the point extraction ventilation in the second part region.

193 The similar methodology of calculating the back-layering length under the longitudinal  
 194 ventilation [4, 10] can be referred to the calculations in this region. Therefore, it is key to  
 195 quantify the smoke characteristics (e.g. the smoke mass flow rate and the temperature) at the  
 196 location of the smoke vent where is the boundary condition of the second part of the back-  
 197 layering length. The details of the equations for calculating the temperature and the mass  
 198 flow rate of the smoke layer will be presented next, following the propagation process as  
 199 shown below.

200 Generally, the movement of the fire smoke in the tunnel is subdivided into several regions  
 201 [18-23]. The process of the smoke spreading is divided into 3 regions in this study, as shown

202 in Fig.2. Regions I and III are the symmetrical ceiling jet region and the one-dimensional  
 203 spreading region, respectively, while region II is the radial spreading and transition region.



204

205 Fig.2 Schematic diagram of smoke spreading in tunnels

206 In Region I, the fire plume rises up from the fire source and propagates horizontally after  
 207 impinging the ceiling. Massive air is entrained from the surrounding atmosphere, because of  
 208 the vertical motion of the buoyant smoke. Thus, the smoke volume increases greatly due to  
 209 the entrainment. According to [24], the mass flow rate of the upwards fire plume is given as:

210 
$$\dot{m}_0 = 0.071\dot{Q}_c^{1/3}H^{5/3} \quad (16)$$

211 When a longitudinal ventilation system operates, the flame of the fire source would be  
 212 deflected, as shown in Fig.3. There is more fresh air entrained into the tilted fire plume than  
 213 before. Consequently, the mass flow rate of the smoke must be modified. Li et al.[25, 26]  
 214 proposed a model to predict the mass flow rate of the tilted fire plume under the effect of the  
 215 longitudinal ventilation,

216 
$$\dot{m}_0 = \begin{cases} 0.3735\dot{Q}_c^{1/3}H_d^{5/3}V^*, & V^* > 0.19 \\ 0.071\dot{Q}_c^{1/3}H_d^{5/3}, & V^* \leq 0.19 \end{cases} \quad (17)$$

217 with 
$$V^* = \frac{V_a}{w^*} \quad (18)$$

218 
$$w^* = \left( \frac{\dot{Q}_c g}{r \rho_0 c_p T_0} \right)^{1/3} \quad (19)$$

219 where  $w^*$  is the characteristic plume velocity,  $V_a$  is the longitudinal velocity,  $V^*$  is the  
 220 dimensionless longitudinal velocity.



222 Fig.3 Flame deflection

223 It is noteworthy that the mass flow rate of the upstream spreading smoke,  $\dot{m}_{up}$ , depends on  
 224 the value of the longitudinal velocity. As such,  $\dot{m}_{up}$  is expressed as:

225 
$$\dot{m}_{up} = \delta \dot{m}_0 \quad (20)$$

226 where  $\delta$  is proportional coefficient, range from 0 to 0.5. Due to lack of experimental data,  
 227 previous studies [17] always take  $\delta = 0.5$  for calculations.

228 The maximum excess ceiling temperature over ambient can be expressed as Eq.21 [26]:

229 
$$\Delta T_{max} = \begin{cases} \frac{\dot{Q}_0}{V_a r^{1/3} H_d^{5/3}}, V^* > 0.19 \\ 17.5 \frac{\dot{Q}_0^{2/3}}{H_d^{5/3}}, V^* \leq 0.19 \end{cases} \quad (21)$$

230 where  $r$  is radius of the fire source.

231 Since the fire plume tilts to the downstream side of the fire source, the position of the  
 232 maximum excess ceiling temperature would be shifted to the downstream of the fire source,  
 233 and its coordinate is written as  $x_0$ , as shown in Fig.1. The displacement is correlated to the tilt

234 angle of the flame. The tilt angle is expressed as follow based on the theory proposed by  
235 Thomas et al.[27]:

$$236 \quad \cos\theta = \begin{cases} 1, & V^* \leq 0.19 \\ (5.26V^*)^{-1/2}, & V^* > 0.19 \end{cases} \quad (22)$$

237 Hence, the coordinate of the reference point (the position of the maximum excess ceiling  
238 temperature) can be written as:

$$239 \quad x_0 = -H_d \tan\theta \quad (23)$$

240 Region II is a transit region. After impinging on the ceiling, the smoke turns to radial  
241 spreading from the reference point until the smoke reaches the side walls of the tunnel. After  
242 that, the one-dimensional smoke spreading in the tunnel longitudinal direction occurs, and the  
243 one-dimensional smoke spreading region is formed. Compared with the one-dimensional  
244 smoke spreading region, the range of the transit region is relatively short, so the friction  
245 between the smoke and the ceiling, the entrainment and the heat loss to the ceiling in the  
246 transit region are all neglected, following the previous studies [18, 19, 21-23, 28]. It is then  
247 reasonable to assume that the heat and the mass remain conservative in the transit region.

248 Region III is a one-dimensional spreading region, and the movement of the smoke can be  
249 easily described by the conservation equations.

250 Thus, the smoke excess temperature decaying along the tunnel from the reference point can  
251 be predicted and a simple model were deduced by Hu [28], given as:

$$252 \quad \frac{\Delta T}{\Delta T_{\max}} = e^{-K(x-x_0)} \quad (24)$$

253 where  $x$  is the coordinate,  $x_0$  is the coordinate of the position of the maximum excess ceiling  
254 temperature,  $\Delta T$  is the smoke excess temperature over ambient in the roof at  $x$ ,  $\Delta T_{\max}$  is the  
255 smoke maximum excess temperature over ambient in the roof (at  $x_0$ );

256  $K$  is the ceiling temperature decay coefficient:

$$257 \quad K = \frac{\alpha D}{c_p \dot{m}_{up}} \quad (25)$$

258 with  $D$  is the length that smoke contact to the tunnel in cross section, it reads

$$259 \quad D = 2h_0 + B \quad (26)$$

260 The entrainment is neglected at this region [18, 19, 28], so the height of ceiling jet is assumed  
261 unchanged. The initial height of the smoke layer in the one-dimension region relates only to  
262 the distance from the surface of the fire source to the ceiling and the width of the tunnel [19,  
263 21, 22], given as:

$$264 \quad h_0 = CH \left( \frac{B}{2H} \right)^{1/3} \quad (27)$$

265 where  $C$  is coefficient constant, ranging from 0.2128 to 0.2483.

266 Further, the heat transfer coefficient,  $\alpha$ , can be also approximately considered as a constant in  
267 the calculation [18]. The same conclusion was also made from the full-scale and model  
268 experiments performed by Hu et al. and Chen et al. [15, 28-30]. Therefore, based on the  
269 Eq.24 introduced above, the temperature distribution of the first part of the smoke back-  
270 layering, the smoke layer between fire source and the smoke vent, can be calculated.  
271 Inserting Eq.25 into Eq.24, the smoke excess temperature at the position of the smoke vent,  
272  $\Delta T_{ex}$ , can be calculated by Eq.28:

$$273 \quad \Delta T_{ex} = \Delta T_{max} e^{-\frac{\alpha D}{c_p \dot{m}_{up}}(d-x_0)} \quad (28)$$

274 It is known that some of the smoke would be removed by the smoke vent, while the residual  
275 spreads over the smoke vent and continue propagating upstream, as shown in Fig.1. Ignoring  
276 the entrainment at Region II and Region III, and based on the mass conservation principle,

277 the mass flow rate of the smoke spreading over the smoke vent,  $\dot{m}_r$ , equals to the initial mass  
 278 flow rate of the smoke spreading upstream,  $\dot{m}_{up}$ , subtracting the amount of the smoke  
 279 extracted by the smoke vent,  $\dot{m}_{ex}$ , given as:

$$280 \quad \dot{m}_r = \dot{m}_{up} - \dot{m}_{ex} \quad (29)$$

281 where  $\dot{m}_{ex}$  can be written as:

$$282 \quad \dot{m}_{ex} = \rho_{ex} V_{ex} A \quad (30)$$

283 It is assumed that the extraction system does not cause the “plug-holing”, which makes the  
 284 smoke spreading over the smoke vent (the second part of the back-layering) staying in one-  
 285 dimensional spreading. Thus, the temperature still decreases exponentially with the tunnel  
 286 length.

287 The back-layering should stop spreading upstream at the place where the static pressure  
 288 balances to the dynamic pressure caused by both the longitudinal ventilation and the point  
 289 extraction ventilation. The position of the smoke stagnation point under the longitudinal  
 290 ventilation can be derived from excess temperature,  $\Delta T_s$ , at the stagnation point as reported  
 291 by Chow et.al [4]. The expression is given as:

$$292 \quad \frac{\Delta T_s}{T_a} = \frac{V'^2}{gh_0} \quad (31)$$

293 It is noteworthy that  $h_0$  is the height of the smoke layer;

294  $V'$  is the modified longitudinal velocity induced by both of the longitudinal ventilation and  
 295 the point extraction ventilation in the roof, given as:

$$296 \quad V' = V_{in} + V_a \quad (32)$$

297 where  $V_a$ ,  $V_{in}$  is the velocity induced by the longitudinal ventilation and the point extraction  
 298 ventilation in the roof respectively. Furthermore,  $V_{in}$  can be obtained by

299 
$$V_{in} = \frac{\dot{m}_{ex}}{2BH\rho_a} \quad (33)$$

300 As illustrated previously, Eq.24 still applies in this region, then Eq.24 converting to Eq.34:

301 
$$\Delta T_s = \Delta T_{ex} e^{-K_1 l'} \quad (34)$$

302 where  $\Delta T_{ex}$  is the excess smoke temperature at the smoke vent, which can be obtained by

303 Eq.28;

304  $K_1$  is the ceiling temperature decay coefficient downstream the smoke vent;

305 
$$K_1 = \frac{\alpha D}{c_p \dot{m}_r} \quad (35)$$

306  $l'$  is the second part of the smoke back-layering length.

307 Substituting Eq.31 into Eq.34 yields

308 
$$\Delta T_{ex} e^{-K_1 l'} = T_a \frac{V'^2}{gh_0} \quad (36)$$

309 Combining Eq.28 and Eq.36, it gets

310 
$$\Delta T_{max} e^{-K(d-x_0)} e^{-K_1 l'} = T_a \frac{V'^2}{gh_0} \quad (37)$$

311 Thus, the second part of the back-layering length,  $l'$ , can be expressed as:

312 
$$l' = -\frac{1}{K_1} \ln \left( \frac{V'^2}{gh_0} \frac{T_a}{\Delta T_{max}} \right) - \frac{K}{K_1} (d - x_0) \quad (38)$$

313 Substituting Eq.17-23, 25-27, 29-30, 32-33, 35 into Eq.38, the second part of the smoke

314 back-layering length can be analytically calculated.

315 Combining two components, the smoke back-layering length finally writes:

316 
$$l = d + l' \quad (39)$$



## 317 4. Results and discussion

### 318 4.1 Comparison to experimental data

319 Since it is not available to conduct validation tests by ourselves in this study, experimental  
320 data of Tang et al., reported in ref. [16], would be used for model validation. First, the  
321 phenomena observed in the tests of Tang et al. [16] are the same as prescribed in the model.  
322 Furthermore, the values for modelling parameters were all measured or quantified in the tests  
323 of Tang et al. [16]. Therefore, experimental data of Tang et al. [16] are available for  
324 validating the present model.

325 The experiments in [16] were conducted in a reduced-scale (a scale of 1/6) model tunnel with  
326 dimensions of 72 m (length)  $\times$  1.5 m (width)  $\times$  1.3 m (height) [14-16]. The fire source  
327 was located at the central of the tunnel. A circular smoke vent (diameter of 0.3 m) was settled  
328 at the middle of the tunnel ceiling. More specifically, it was installed 1 m upstream the fire  
329 source ( $d=1$  m). A longitudinal ventilation system was also installed at the entrance of the  
330 tunnel model. The parameters, including the heat release rate of the fire source, the exhaust  
331 velocity and the longitudinal velocity, were variables in the tests. The smoke back-layering  
332 lengths were derived from the measured ceiling temperature distributions in the experiments.  
333 The thermocouples were arranged at an interval of 0.5 m.

334 Table.1 Summary of valid scenarios in the experiments [16]

Test No.	Heat release rate (kW)	Exhaust velocity (m/s)	Longitudinal velocity (m/s)
1~9	30	0.5, 1, 1.5, 2, 2.2	0.3, 0.5
10~18	40	0.5, 1, 1.5, 2, 2.2	0.3, 0.5
19~27	50	0.5, 1, 1.5, 2, 2.2	0.3, 0.5

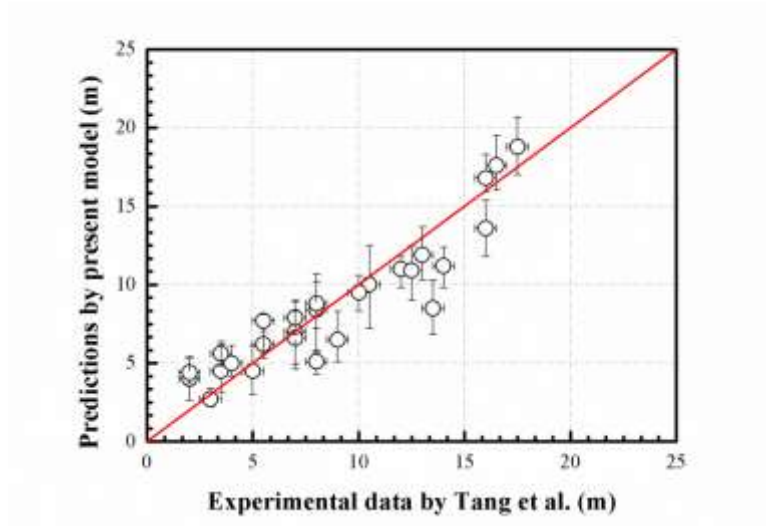
335 Recall that the present model applies to one smoke vent immersed inside the smoke back-  
336 layering which implies that the back-layering length is longer than the distance from the  
337 smoke vent to the fire source  $d$  and no plug-holing occurs, as shown in Fig.1. Therefore, the  
338 available experimental data from [16] used for illustrating the accuracy of the model are the  
339 back-layering lengths longer than 1 m, as the smoke vent in the roof is located 1 m upstream  
340 the fire source in the experimental configuration [16]. Table 1 summarises the information of  
341 the experiments used for comparing.

342 Before illustrating the agreement that is obtained between predictions and experiments, there  
343 needs to quantifying the uncertainty in the measured output quantities ( $l$ ) and input quantities  
344 ( $\dot{Q}_0, V_a, V_{ex}$ ). The latter component attributes to the propagation of input parameter  
345 uncertainty respectively. As the thermocouples were arranged at an interval of 0.5 m to  
346 quantify the smoke back-layering length,  $l$ , the uncertainty of the measurements of  $l$  is  
347  $\pm 0.5$  m. Additionally, the heat release rate of the fire source was controlled by a gas flow  
348 meter with accuracy of  $\pm 0.1$  m<sup>3</sup>/h [14-16]. Thus, the relatively uncertainty in HRR  
349 measurement can be roughly calculated to be 8%. Both the longitudinal velocity and the  
350 pointed exhaust velocity were measured by a digital hot-wire anemometer. Due to lack of  
351 details of the hot-wire anemometer, the measurement uncertainties of the velocity are  
352 estimated as 3%, according to the work reported by F.E. Jørgensen [31].

353 Based on the uncertainty analysis above, comparisons of the predictions from the present  
354 model to experimental data of Tang et al. [16] are provided in Fig.5 The horizontal  
355 uncertainty bar represents uncertainty in the experiment measurement of the back-layering  
356 length while the vertical bar represents the propagation of input parameter uncertainty  
357 resulting from the uncertainty in the HRR, longitudinal velocity and exhaust velocity. The  
358 diagonal line with a slope of 1 is employed to evaluate the discrepancy between the model

359 predictions and the experimental data. Clearly, all the results are concentrated along the line  
360 and a general satisfactory agreement is observed.

361



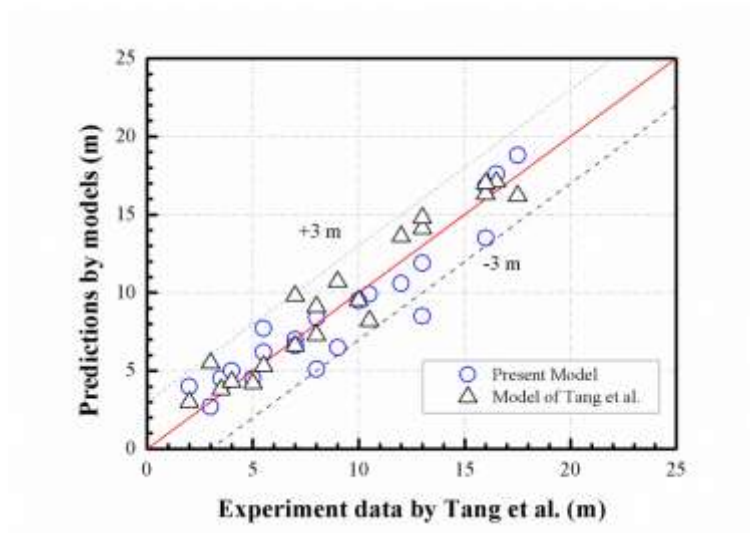
362

363 Fig.5 Comparison of the predictions with the experimental results in [16]

364 The horizontal uncertainty bar and vertical uncertainty bar represents uncertainty in the  
365 experiment measurement of the back-layering length and the propagation of input parameter  
366 uncertainty respectively.

#### 367 **4.2 Comparison to other model results**

368 As described in the introduction section, the model of Tang et al. [16] is the only existing  
369 model for predicting the smoke back-layering for the conditions of the longitudinal ventilated  
370 tunnel with the smoke vent in the roof upstream the fire source. Although it is not a  
371 straightway to verify the present model by comparing to another model, it is still interesting  
372 to make this kind of comparisons in this section as the two models were developed by two  
373 different methodologies, as introduced previously.



374

375

Fig.6 Comparison to the results calculated by the model of Tang et al.

376

The results calculated by the model of Tang et al. [16] and the present model are illustrated in

377

Fig.6. The abscissa is the back-layering length measured in the experiments, while its

378

ordinate is the results predicted by the two models. The circles represent the predictions of

379

the present model, and the triangles represent the predictions of the other model. Fig. 6 shows

380

that the predicted plots are closed to the diagonal line with a slope of 1. Two dash lines are

381

drawn with the offset of 3 m to display the deviation between the predictions of the models

382

and the experimental data. It is clear that the predictions of both models are almost located

383

between these two dash lines, which means the deviations of both predictions are less than 3

384

m. So the plots from both models are closed to each other.

385

Although Figure 6 shows the two models give similar predictions, a discussion is necessary

386

on the difference of two models. As illustrated previously, the two models were developed by

387

two different approaches. The model of Tang et al. incorporates the effect of the point

388

extraction ventilation on the length of back-layering via a reduced heat release rate of the fire

389

source,  $\dot{Q}^{**}$ , from the point view of the heat conservation. As a result, the model of Tang et al.

390

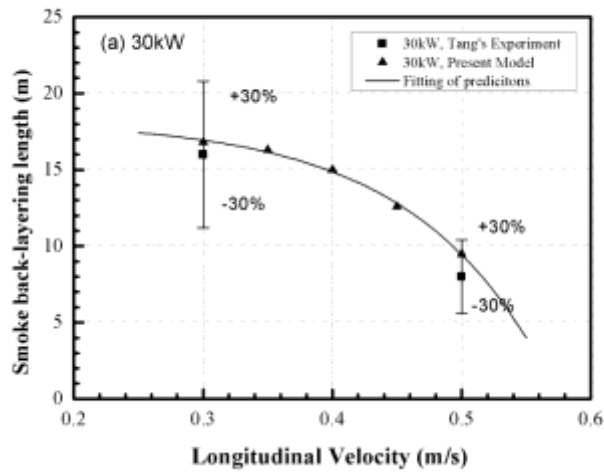
for quantifying the length of back-layering, as shown in Eq. 9, is only associated with  $\dot{Q}^{**}$

391 and  $\dot{V}^{**}$ . The detailed mass and heat transfer along the smoke back-layering was not taken  
392 into account. The present model, by contrast, incorporates much more of fire smoke spread  
393 details, ceiling jets, and mass flow rate calculations than does the existing model. For  
394 example, the smoke back-layering described in the present model is divided by the smoke  
395 vent location into two regions, each of which is resolved by including the mechanism from  
396 the mass and heat conservations principles. As a consequence, one benefit of the present  
397 model is able to explicitly explore the impact of the smoke vent location on the back-layering  
398 length (see section 4.4). Additionally, the present model is ambitious and convenient to be  
399 further developed to a universal model to predict the back-layering length in the  
400 longitudinally ventilated tunnel with multiple smoke vents activated.

### 401 **4.3 Prediction of the back-layering length under different ventilation condition**

402 Experimental data in [16] show that the smoke back-layering length is dramatically  
403 influenced by the longitudinal ventilation velocity as well as the velocity of the point  
404 extraction ventilation in the roof. In this section, more results are calculated by the present  
405 model to supplement the experimental data to discuss the influences of the two kinds of  
406 ventilations on the smoke back-layering lengths.

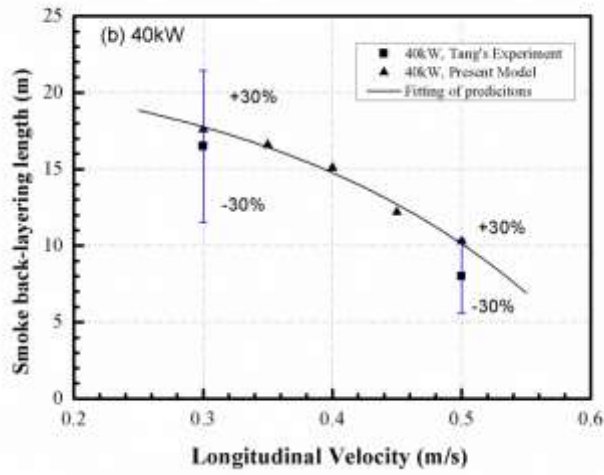
#### 407 **4.3.1 Different longitudinal ventilation velocity**



408

409

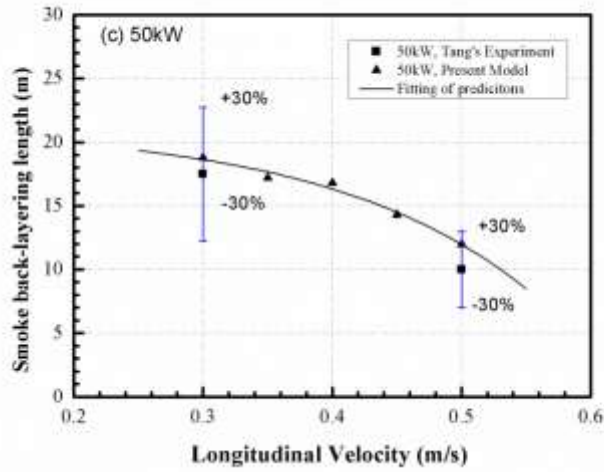
(a)



410

411

(b)



412

(c)

Fig.7 The smoke back-layering lengths varying with different longitudinal velocities

( $V_{ex} = 1.0 \text{ m/s}$ ) (a): HRR=30 kW; (b): HRR=40 kW; (c); HRR=50 kW.

The predictions of the smoke back-layering length with different longitudinal velocities are compared to the experimental results measured in [16], as shown in Fig.7. The exhaust velocity is set at  $1.0 \text{ m/s}$  in all tests. Fig.7 (a), (b) and (c) represents 30 kW, 40 kW and 50 kW heat release rate respectively. The curves displayed in Fig.7 are drawn by fittings of the predictions, while the rectangles present the experimental results.

The prediction curves in Fig.7 just well captured the similar tendency of the smoke back-layering length varying with the longitudinal velocity as observed in the experiments. The prediction error is less than 30%. It is logical that the prediction of the fire smoke back-layering length gets shorter as the longitudinal velocity becomes larger. Indeed, the increase of the dynamics pressure with the longitudinal velocity can suppress the fire smoke spreading upstream.

Fig. 7 also shows the good predictions of the smoke back-layering lengths for different HRRs. When the heat release rate grows, the fire smoke back-layering length becomes larger. Indeed, the increase of the smoke buoyancy momentum with HRR would increase the back-layering length, which has been well explained by Eq. 21 and Eq. 38.

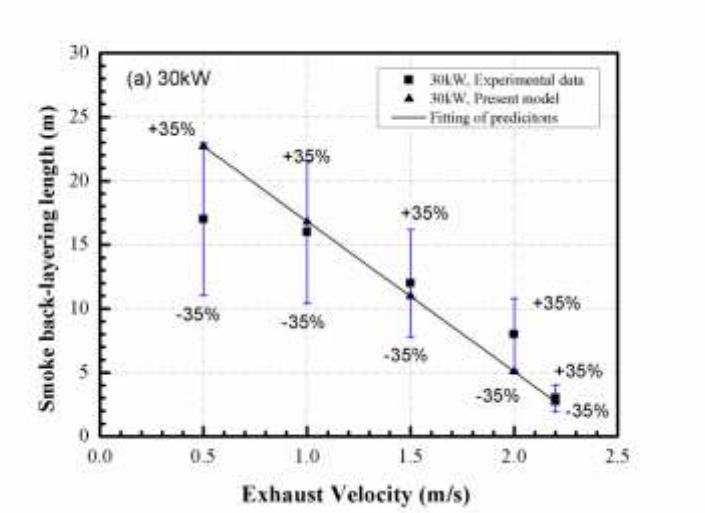
#### 4.3.2 Different exhaust velocity through the smoke vent in the roof

In order to show the impact of the ceiling smoke exhaust velocity on the smoke back-layering length, Fig. 8 is drawn to show the variations of the predictions of the back-layering length with different exhaust velocities. The experimental results are also presented in Fig. 8 for the purpose of comparison. The longitudinal velocity is  $0.3 \text{ m/s}$  for all cases. All the three heat release rates in the experiments (30 kW, 40 kW and 50 kW) are considered. The exhaust

437 velocity increases from  $0.5\text{ m/s}$  to  $2.2\text{ m/s}$ , referring to the exhaust velocity range in the  
438 experiments. The curves in the Fig.8 are determined by fittings of the predictions, while the  
439 plots present the experiments results.

440 Clearly, the experimental results show that increase of exhaust velocity would reduce the  
441 smoke back-layering length, e.g. keeping the fire heat release rate of  $30\text{ kW}$  and the  
442 longitudinal velocity of  $0.3\text{ m/s}$  constant, the back-layering length decreases from  $17\text{ m}$  to  
443  $3.5\text{ m}$ , when the exhaust velocity grows from  $0.5\text{ m/s}$  to  $2.2\text{ m/s}$ . Less smoke spread to the  
444 upstream side in larger exhaust velocity due to more smoke removed by the extraction system,  
445 so that the residual smoke can be more easily suppressed by the longitudinal air flow. In  
446 addition, Fig. 7 also illustrates the accuracy of the present model in predicting the smoke  
447 back-layering lengths for different HRR and exhaust velocity.

448 It notes that the lines fitting by the predictions are straight line while it is not the case for the  
449 experimental plots, resulting in moderate gaps between the predictions and the experimental  
450 results (but still less than 35%). The reason is that the effect of the point extraction ventilation  
451 on the fire plume, which is confirmed in [16] due to the short distance between the fire source  
452 and the smoke vent, is not considered in the present model at this research stage. Further  
453 work about the interaction between the fire plume and the extraction system are needed.

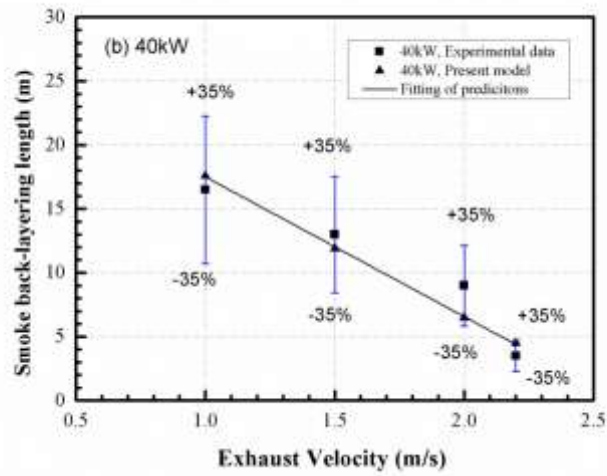


454



455

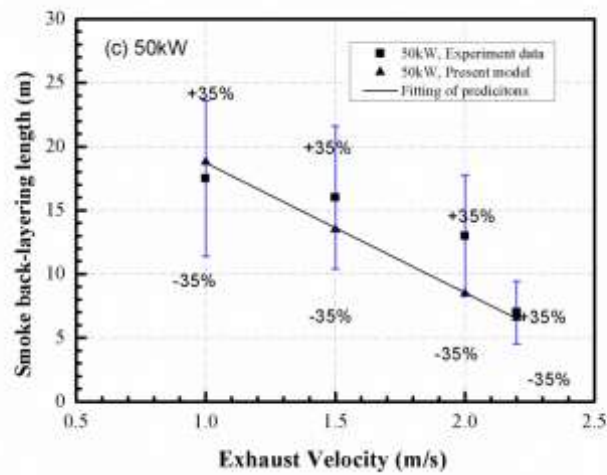
(a)



456

457

(b)



458

(c)

Fig.8 The smoke back-layering lengths variation with different exhaust velocities

459

460

461

$$(V_a = 0.3 \text{ m/s})$$

462

#### 4.4 Prediction of the back-layering length for different smoke vent location

463

Because the temperature of the removed smoke is related to the position of the smoke vent

464

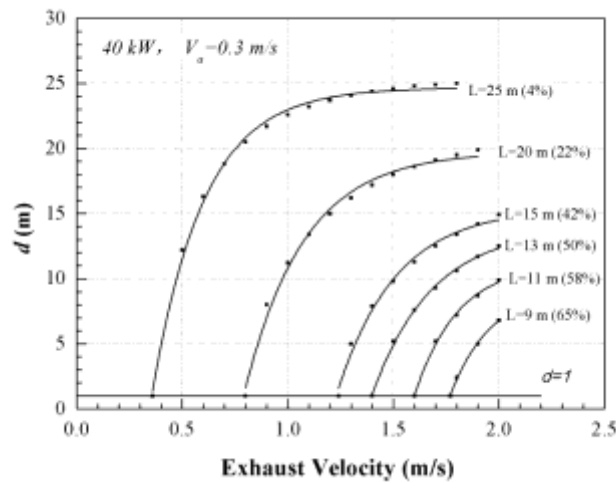
away from the fire source,  $d$  should have apparent impact on the smoke back-layering length

465

in the tunnel fire. It is significant to use the present model to show and discuss the influence

466 of the distance  $d$  on the back-layering length. Changing the upstream position of the smoke  
467 vent, the smoke back-layering lengths are calculated by the present model. One heat release  
468 rates ( $40\text{ kW}$ ) and two longitudinal velocities ( $0.3\text{ m/s}$ ,  $0.5\text{ m/s}$ ) and a range of exhaust  
469 velocities are considered. The results are shown in Fig.9.

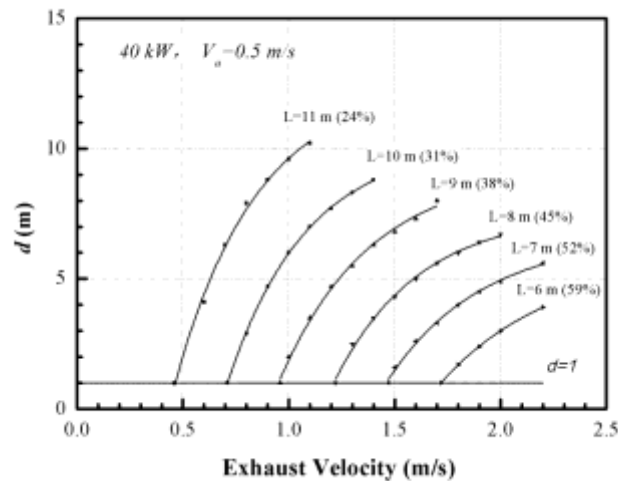
470 In Fig.9, every single curve represents a certain value of the back-layering length with  
471 different  $V_{ex}$  and  $d$ . The percentage for each curve as shown in Fig. 9, named as “reduction  
472 percentage” here, is one minus the ratio of the back-layering length under both of the  
473 longitudinal ventilation and the point extraction ventilation to that only under the longitudinal  
474 ventilation.



475

476

(a)



(b)

Fig.9 Predictions of the smoke back-layering lengths varying with different smoke vent position

(a)  $V_a = 0.3 \text{ m/s}$  (b)  $V_a = 0.5 \text{ m/s}$

Fig.9(a) shows the curves under the condition of  $V_a = 0.3 \text{ m/s}$ , presenting the values of the back-layering length range from 9 m to 25 m. Despite of the difference in the coordinates and scales, the curves are similar to each other in tendency. It is clear to see that the back-layering length decrease as shortening the distance  $d$  and raising the exhaust velocity  $V_{ex}$ . It is not surprise to see this tendency because the smoke vent closer to the fire source with a larger exhaust velocity could exhaust larger amount of the smoke with higher temperature out of the tunnel, then resulting in reducing the buoyancy force of the back-layering. Particularly, when the distance  $d$  is larger than 15 m, the maximum reduction percentage of the back-layering length is less than 42% in this phenomenon, no matter how large the exhaust velocity is. With the decrease of  $d$ , the maximum reduction percentage would increase as well. For example, the maximum reduction percentage of the back-layering length would increase to 65% when  $d = 7 \text{ m}$ . It should also be highlighted that the distance  $d$  plays a more important role in reducing the back-layering length when the exhaust velocity is large. For example, when the

495 exhaust velocity is smaller than  $0.8 \text{ m/s}$ , the reduction percentage of the back-layering length  
496 is ranged from 0% to 22% (0% happens when  $d$  is larger than the back-layering length, and  
497 22% happens when  $d = 0 \text{ m}$ ); When the exhaust velocity is larger than  $1.75 \text{ m/s}$ , the  
498 reduction percentage of the back-layering length is ranged from 0% to 65% (0% happens  
499 when  $d$  is larger than the back-layering length, and 65% happens when  $d = 0 \text{ m}$  ).

500 Fig.9 (a) also appears the correlations between the exhaust velocity and the back-layering  
501 length. For the curves of  $l = 15 \text{ m}$ ,  $l = 13 \text{ m}$ ,  $l = 11 \text{ m}$ , and  $l = 9 \text{ m}$ , the distances between  
502 adjacent curves almost equals to each other. Introducing a straight line of  $d = 1 \text{ m}$ , there are  
503 several points of intersection with these curves, representing the exhaust velocities for each  
504 back-layering length when  $d = 1 \text{ m}$ . It is interesting to note that the back-layering length  
505 linearly increase with the exhaust velocity, corresponding to the conclusions in section 3.3.2.

506 Fig.9(b) illustrates the curves of then back-layering lengths when the longitudinal velocity  
507 increase to  $0.5 \text{ m/s}$ . The same tendencies, as described above, are also observed here.  
508 However, compared to the curves with  $0.3 \text{ m/s}$  longitudinal velocity, as shown in Fig. 9(a),  
509 the  $d$  corresponding to a certain maximum reduction percentage in these phenomena is much  
510 smaller. For instance,  $d = 15 \text{ m}$  in the tests with  $0.3 \text{ m/s}$  longitudinal velocity corresponding  
511 to 42% maximum reduction percentage, whereas about  $d = 8 \text{ m}$  in the tests with  $0.5 \text{ m/s}$   
512 longitudinal velocity corresponding to the same maximum reduction percentage. As  
513 discussed above, keeping other conditions constant, a smaller distance from the smoke vent  
514 to the fire source is expected to obtain a certain maximum reduction percentage as the  
515 longitudinal velocity increases.

## 516 **5. Conclusions**

517 In the paper at hand, an analytical model has been developed for quantifying the fire smoke  
518 back-layering length in tunnel with a combination of the longitudinal ventilation and the  
519 point extraction ventilation in the roof from first principles. Contrast to the existing models, a  
520 different approach has been applied in the model development. More importantly, the mass  
521 flow rate during the whole spread process of back-layering is cooperated in the present model.  
522 The model can be solved analytically with the input quantities (the heat release rate of fire  
523 source, the longitudinal velocity, the exhaust velocity, the width and height of the tunnel, the  
524 distance of the smoke vent to the fire source and the area of the smoke vent).

525 The accuracy of the model as presented has been illustrated by means of an experimental data  
526 set [16]. A comparison between of the present model and the model of Tang et al. [16] has  
527 also been made to see the comparability of the two models. Generally, satisfactory  
528 agreements have been obtained.

529 Extensive model predictions on the back-layering length, varying the velocity of the  
530 longitudinal ventilation, the exhaust velocity and the position of the smoke vent in the roof,  
531 have been done to illustrate its trends. The prediction of the back-layering length gets shorter  
532 as the longitudinal velocity or the exhaust velocity becomes larger, which is consistent with  
533 these phenomena in reality. It is interesting to note that the prediction of the back-layering  
534 length linearly increases with the decrease of the exhaust velocity, although the limited  
535 number of points in the tests at hand show more or less nonlinear trend.

536 Another important phenomenon discussed is that shortening the distance between the smoke  
537 vent and the fire source benefits shortening the back-layering length. The reduction of the  
538 back-layering length is more pronounced for higher exhaust velocity. It is also highlighted

539 that a smaller distance from the smoke vent to the fire source is expected to obtain a certain  
540 maximum reduction percentage as the longitudinal velocity increases.

541 Since the analytical model at this research stage is simple, it is important to recall its  
542 limitations in order to avoid improper use. The model is only valid for the phenomenon that  
543 one smoke vent set upstream of the fire source combined with the longitudinal ventilation, as  
544 described in Fig. 1. Furthermore, the plug-holing phenomenon happening at the smoke vent is  
545 not in the application scope of the present model. Additionally, due to the interactions  
546 between the fire plume and the smoke vent was not considered in the present model, some  
547 error would be expected as the smoke vent near the fire source. In the future, based on the  
548 present model, more comprehensive model would be studied and developed by considering  
549 more smoke vents operated in the tunnel fire, the plug-holing phenomenon as well as the  
550 interactions between the fire plume and the smoke vent in the model.

## 551 Acknowledgements

552 This work is jointly supported by Natural Science Funds of China [Grant No. 51576144 and  
553 No. 51508426] and China Scholarship Council [Grant No.201506270067].

## 554 Reference

- 555 [1]. A.Hacck, *Fire Protection in Traffic Tunnels General Aspects and Results of the EUREKA*  
556 *Project*. Tunnelling and Underground Space Technology, 1998. **13**(4): p. 5.
- 557 [2]. F. Vuilleumier, A.W., B. Crausaz, *Safety aspects of railway and road tunnel example of the*  
558 *lotschberg railway tunnel and mont-blanc road tunnel*. Tunnelling and Underground Space  
559 *Technology*, 2002. **17**.
- 560 [3]. Leitner, A., *The fire catastrophe in the Tauern Tunnel-experience and conclusions for the*  
561 *Austrian guidelines*. Tunnelling and Underground Space Technology, 2001. **16**: p. 217-223.
- 562 [4]. Chow, W.K., et al., *Smoke movement in tilted tunnel fires with longitudinal ventilation*. *Fire*  
563 *Safety Journal*, 2015. **75**: p. 14-22.
- 564 [5]. J.P.Vantelon, et al. *Investigation of fire-induced smoke movement in tunnels and stations: an*  
565 *application to the Paris Metro*. in *Proceedings of the Third International Symposium on Fire*  
566 *Safety Science*. 1991. Edinburgh,UK: Elsevier.

- 567 [6]. Li, Y.Z., B. Lei, and H. Ingason, *Study of critical velocity and backlayering length in*  
568 *longitudinally ventilated tunnel fires*. Fire Safety Journal, 2010. **45**(6-8): p. 361-370.
- 569 [7]. P.Deberteix, D.Gabay, and D.Blays. *Experimental study of fire-induced smoke propagation in a*  
570 *tunnel in the presence of longitudinal ventilation*. in *Proceedings of the International*  
571 *Conference on Tunnel Fires and Escape from Tunnels*. 2001. Washington.
- 572 [8]. P.H.Thomas, *The movement of buoyant fluid against a stream and venting of underground*  
573 *fires*, in *Fire Research Note*. 1958, Fire Research Station: Watford, UK.
- 574 [9]. Kurioka, H., et al., *Fire properties in near field of square fire source with longitudinal*  
575 *ventilation in tunnels*. Fire Safety Journal, 2003. **38**(4): p. 319-340.
- 576 [10]. Hu, L.H., R. Huo, and W.K. Chow, *Studies on buoyancy-driven back-layering flow in tunnel*  
577 *fires*. Experimental Thermal and Fluid Science, 2008. **32**(8): p. 1468-1483.
- 578 [11]. O. Vauquelin, O.M., *Smoke extraction experiments in case of fire in a tunnel*. Fire Safety  
579 Journal, 2002. **37**: p. 9.
- 580 [12]. O. Vauquelin, D.T., *Definition and experimental evaluation of the smoke "confinement*  
581 *velocity" in tunnel fires*. Fire Safety Journal, 2005. **40**(4): p. 320-330.
- 582 [13]. Ingason, H. and L. Ying Zhen, *Model scale tunnel fire tests with point extraction ventilation*.  
583 Journal of Fire Protection Engineering, 2011. **21**(1): p. 5-36.
- 584 [14]. Chen, L.F., et al., *Studies on buoyancy driven two-directional smoke flow layering length with*  
585 *combination of point extraction and longitudinal ventilation in tunnel fires*. Fire Safety  
586 Journal, 2013. **59**: p. 94-101.
- 587 [15]. Chen, L.F., et al., *Thermal buoyant smoke back-layering flow length in a longitudinal*  
588 *ventilated tunnel with ceiling extraction at difference distance from heat source*. Applied  
589 Thermal Engineering, 2015. **78**: p. 129-135.
- 590 [16]. Tang, F., et al., *Thermal smoke back-layering flow length with ceiling extraction at upstream*  
591 *side of fire source in a longitudinal ventilated tunnel*. Applied Thermal Engineering, 2016.  
592 **106**: p. 125-130.
- 593 [17]. Yao, Y., et al., *Smoke back-layering flow length in longitudinal ventilated tunnel fires with*  
594 *vertical shaft in the upstream*. Applied Thermal Engineering, 2016. **107**: p. 738-746.
- 595 [18]. J.P.Kunsch, *Critical velocity and range of a fire-gas plume in a ventilated tunnel*. Atmospheric  
596 Environment, 1999. **33**: p. 13-24.
- 597 [19]. J.P.Kunsch, *Simple model for control of fire gases in a ventilated tunnel*. Fire Safety Journal,  
598 2002. **37**: p. 67-81.
- 599 [20]. Delichatsios, M.A., *The flow of fire gases under a beamed ceiling*. Combustion and Flame,  
600 1981. **43**: p. 1-10.
- 601 [21]. Oka, Y., H. Oka, and O. Imazeki, *Ceiling-jet thickness and vertical distribution along flat-*  
602 *ceilinged horizontal tunnel with natural ventilation*. Tunnelling and Underground Space  
603 Technology, 2016. **53**: p. 68-77.
- 604 [22]. Oka, Y. and H. Oka, *Velocity and temperature attenuation of a ceiling-jet along a horizontal*  
605 *tunnel with a flat ceiling and natural ventilation*. Tunnelling and Underground Space  
606 Technology, 2016. **56**: p. 79-89.
- 607 [23]. Li, S., et al., *Theoretical and experimental analysis of ceiling-jet flow in corridor fires*.  
608 Tunnelling and Underground Space Technology, 2011. **26**(6): p. 651-658.
- 609 [24]. Drysdale, D., *An Introduction to Fire Dynamics*. Third ed. 2011, United Kingdom: John Wiley  
610 & Sons Ltd. 132-138.
- 611 [25]. Li, Y.Z. and H. Ingason, *The maximum ceiling gas temperature in a large tunnel fire*. Fire  
612 Safety Journal, 2012. **48**: p. 38-48.
- 613 [26]. Li, Y.Z., B. Lei, and H. Ingason, *The maximum temperature of buoyancy-driven smoke flow*  
614 *beneath the ceiling in tunnel fires*. Fire Safety Journal, 2011. **46**(4): p. 204-210.
- 615 [27]. Raj, P.K., et al., *Experiments Involving Pool and Vapor Fires from Spills of Liquefied Natural*  
616 *Gas on Water*. 1979: U.S. Coast Guard, Office of Research and Development.

- 617 [28]. Hu, L.H., et al., *Full-scale burning tests on studying smoke temperature and velocity along a*  
618 *corridor*. Tunnelling and Underground Space Technology, 2005. **20**(3): p. 223-229.
- 619 [29]. Hu, L.H., L.F. Chen, and W. Tang, *A global model on temperature profile of buoyant ceiling*  
620 *gas flow in a channel with combining mass and heat loss due to ceiling extraction and*  
621 *longitudinal forced air flow*. International Journal of Heat and Mass Transfer, 2014. **79**: p.  
622 885-892.
- 623 [30]. Hu, L.H., et al., *A non-dimensional global correlation of maximum gas temperature beneath*  
624 *ceiling with different blockage–fire distance in a longitudinal ventilated tunnel*. Applied  
625 Thermal Engineering, 2013. **56**(1-2): p. 77-82.
- 626 [31]. Jørgensen, F.E., *How to Measure Turbulence with Hot- Wire Anemometers, a Practical Guide*.  
627 2002, Denmark: Dantec Dynamics.
- 628